Most suitable mother wavelet for the analysis of fractal properties of stride interval time series via the average wavelet coefficient

Zhenwei Zhang* Jessie VanSwearingen† Jennifer S. Brach Subashan Perera‡
Ervin Sejdić

Abstract

Human gait is a complex interaction of many nonlinear systems and stride intervals exhibit self-similarity over long time scales that can be modeled as a fractal process. The scaling exponent represents the fractal degree and can be interpreted as a biomarker of relative diseases. The previous study showed that the average wavelet method provides the most accurate results to estimate this scaling exponent when applied to stride interval time series. The purpose of this paper is to determine the most suitable mother wavelet for the average wavelet method. This paper presents a comparative numerical analysis of sixteen mother wavelets using simulated and real fractal signals. Simulated fractal signals were generated under varying signal lengths and scaling exponents that indicate a range of physiologically conceivable fractal signals. The five candidates were chosen due to their good performance on the mean square error test for both short and long signals. Next, we comparatively analyzed these five mother wavelets for physiologically relevant stride time series lengths. Our analysis showed that the symlet 2 mother wavelet provides a low mean square error and low variance for long time intervals and relatively low errors for short signal lengths. It can be considered as the most suitable mother function without the burden of considering the signal length.

Keywords: fractals, time series analysis, self similarity, gait, stride intervals, wavelets , 1/f process, mother wavelet.

*Zhenwei Zhang and Ervin Sejdić are with the Department of Electrical and Computer Engineering, Swanson School of Engineering, University of Pittsburgh, Pittsburgh, PA, 15261, USA. E-mail: esejdic@ieee.org. Ervin Sejdić is the corresponding author.

†Jessie Van Swearingen and Jennifer S. Brach are with the Department of Physical Therapy, University of Pittsburgh, Pittsburgh, PA, 15260, USA.

‡Subashan Perera is with the Department of Medicine, Division of Geriatrics, University of Pittsburgh, Pittsburgh, PA, 15261, USA.

1 Introduction

Walking is the most common mode of human movement [1] and human gait involves the complex interactions of many nonlinear systems [2]. Disease, aging, trauma and genetic disorders can all have significant effects on human gait [3, 4, 5]. The locomotor system is a functional composite system of a number of body systems. The composite system is the integration of contributions from the central nervous, musculoskeletal, cardiopulmonary and metabolic systems. Specific central nervous system input from the cerebellum, motor and premotor cortices, and the basal ganglia, as well as peripheral feedback from visual, vestibular and proprioceptive sensors lead to adjustments and adaptations of locomotor system function relative to internal and external conditions [2, 6]. In a healthy subject, the stride intervals display long-range power-law correlation, which may be the result of peripheral input or lower motorneuron control, or of the walking rhythm as controlled by higher nervous system centers [7].

Stride interval times series possess complex statistical properties [6, 7, 4, 8]. Variance in healthy stride interval is not truly random and possesses temporal structure from one stride to the next [7, 4]. Stride interval demonstrates fractal characteristics meaning that the stride to stride variations over a few strides are similar to those over hundreds of strides [4, 9, 10]. Fractal processes can be used to describe the natural irregularity of gait process because of temporal correlation [8].

Neurophysiological changes may alter the stride-interval correlations. Advanced age is an example of one condition known to affect neurophysiology and impact gait. These effects include decreased nerve conduction velocity, loss of motoneurons, decreased reflexes, reduced muscle strength, decreased proprioception and reduced central processing capabilities [7]. Parkinson's disease and Huntington's disease are neurodegenerative disorders of the central nervous system that produce pathological changes in the basal ganglia. These changes in basal ganglia may be associated with diminished stride-interval correlations associated with these disorders [7]. Amyotrophic lateral sclerosis affects the motoneurons of the cerebral cortex, brain stem, and spinal cord, and has been related to changes in walking speed [4]. A commonality seen in all of these neurodegenerative conditions and diseases has been an increase in the stride interval time and the magnitude of fluctuation as related to the fractal [7, 4].

Many studies have showed the fractal properties of stride interval time series in different pathologies such as amyotrophic lateral sclerosis [4], Huntingtons disease[4, 7], and Parkinsons disease [11, 12]. Most of studies are based on Detrended Fluctuation Analysis (DFA). For example, the presence of fractal properties in gait during auditory cues was revealed using the DFA method [13].

In [14], authors controlled the movements of subjects and reinterpreted DFA of minimizing the stride-to-stride variations in walking speed. Certain recent works focus on using machine learning techniques, such as support vector machine and hidden Markov model, for different gait patterns recognition and disease diagnosis [15, 16, 17, 18, 19]. Wavelet-based signal projection was also applied for classifying gait signals of certain neurological disorders [20]. Some other works in this direction differentiated patients with neurodegenerative diseases using phase synchronization and conditional entropy [21] .

It has been shown that stride intervals represent a stochastic process with power spectral density equal to $S(f) = \frac{C_\omega}{|f|^\beta}$ [22]. β value can be estimated in the time domain using techniques such as dispersional analysis, bridge detrended scaled window variance and detrended fluctuation analysis [23, 24], in the frequency domain by using the ${}^{low}PSE_{we}$ method [25], and in the time-scale domain with the average wavelet coefficient (AWC) method [26]. Previous contributions have shown that the AWC method shows a uniform performance for the range of fGn and fBm class signals [6].

The purpose of this paper is to determine the most suitable mother wavelet for the average wavelet coefficient method to accurately estimate the β exponent in $1/f^\beta$ processes and to highlight the limitations of these mother wavelets. The tests include the $1/f^\beta$ process which is the best indicator of simulated signals of physiological processes. To achieve our goal, we used simulated $1/f^\beta$ processes with characteristics similar to stride interval time series, and we also used stride interval time series obtained from several patient groups [27].

2 Methodology

2.1 $1/f^\beta$ Processes

The $1/f^\beta$ processes are statistically self-similar random processes that generally have an inverse power relationship between measured power spectra and frequency $S(f) = 1/f^\beta$ [27, 28, 29, 30, 31, 32, 33]. In general, the $1/f^\beta$ proccesses are classified into two different models: fractional Brownian motion (fBm) and fractional Gaussian noise (fGn), as proposed by Kolmogorov [27, 33, 34]. Fractional Brownian motions are processes corresponding to $1 < \beta < 3$, where $\beta = 2$ represent the Wienner process, which entails classical Brownian motion. The fractal Gaussian noise represents processes corresponding to $-1 < \beta < 1$, while $\beta = 0$ is stationary white Gaussian noise that has a flat spectrum [27, 33]. The two models are degenerated at the boundary where $\beta = -1$, $\beta = 1$, $\beta = 3$ [33]. The fractional Brownian motion process is nonstationary with stationary increments,

while the Gaussian noise process is stationary [33, 28, 27]. The probability distribution of fGn signal is independent of segment length and position [27]. For the fBm signal, the probability distribution in the short sampled segment is equal to the long segment when the long segment is rescaled [27]. There is infinite low-frequency power for fractional Brownian motion that has finite power in any finite time interval and for the fractional Gaussian noise there is infinte high-frequency power [33, 35]. The cummulative summation of the nonstationary fBn signals results in fGn signals [27, 36, 33]

The Hurst exponent can be estimated by the average wavelet coefficient method. The Hurst exponent is a parameter related to the fractal dimension, which represents the smoothness of a time series [37]. The relationship between Hurst Exponent and the fractal dimension is given as the followings: $D = 2 - H$, where the range of H is $0 < H < 1$. The relationship between each class's Hurst exponent and $1/f^{\beta}$ is [38]:

$$\begin{aligned} H_{fGn} &= \frac{\beta + 1}{2} \\ H_{fBm} &= \frac{\beta - 1}{2} \end{aligned} \tag{1}$$

The Hurst exponent can be denoted as H_{fGn} and H_{fBm}, and the processes differ in significant ways corresponding to $0 \leq H \leq 0.5$, $H = 0.5$, and $0 \leq H \leq 1$ [34]. $H = 0.5$ is the special case, here $H_{fGn} = 0.5$ means white Gaussian noise and $H_{fBm} = 0.5$ is Brownian motion. $H_{fGn} < 0.5$ is anti-correlated Gaussian noise while $H_{fGn} > 0.5$ is correlated noise [28]. $H_{fBm} < 0.5$ is anti-persistent Brownian motion while $H_{fBm} < 0.5$ is persistent Brownian motion [28]. From the equations we gather that $\beta = 0$ is white Gaussian noise, $\beta = 1$ is pink noise, and $\beta = 2$ is Brownian motion.

The concept of fractals can be used to model certain aspects of physiological dynamics such as fractal lungs, blood pressure, walking and hearts [7, 23, 39, 40, 41]. Healthy heart rate, blood pressure and walking produce pink noise in the output signal. These noises lose their $1/f$ characteristics due to age and disease, becoming either white or Brownian [22, 42, 43]. For example, the gait of patients with Parkinson's disease has stochastic behavior similar to the Brownian process [22, 44].

2.2 Estimating β values via the average wavelet coefficient method

The wavelet transform maps the time domain waveforms into a frequency-time domain and estimates the signals both in the both time and frequency domains [**?**, 45]. The main idea of wavelet transform is to compare the similarity between an original waveform and the basic function called

mother wavelet. The calculation of a process generates a dilated and translated version of the mother wavelet and the process of calculations performed at every scale and time point represents the continuous wavelet transform, which is usually used to study the fractal process [5]. The wavelet is donated by a scale parameter a and a translation parameter b, where a is a positive number and b is a real number. The wavelet basis can be given by a single function called mother function [46]:

$$\psi_{a;b}(x) = \psi(\frac{x-b}{a}) \tag{2}$$

The continuous wavelet transform is given as

$$W[h](a,b) = \frac{1}{\sqrt{a}} \int_{-\infty}^{\infty} \psi^*_{a;b}(x) h(x) dx \tag{3}$$

Mother wavelet represents the basic function for the wavelet transform as does the sine in the Fourier transform. Figure 1 illustrates some commonly used mother functions in our experiments [47].

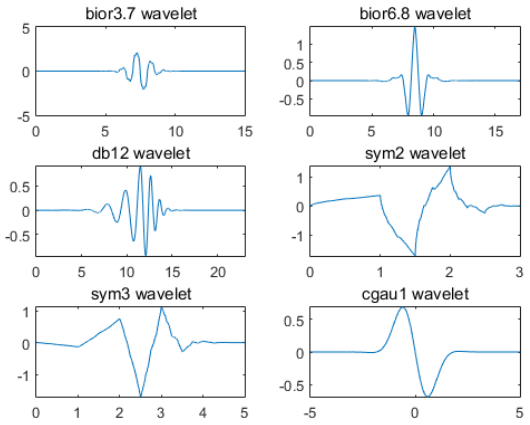

Figure 1: Example mother wavelets used in our experiments.

The average wavelet coefficient method is used to estimate the Hurst exponents. To find the Hurst transform, the data is transformed into the wavelet domain by using wavelet and the arithmetic mean is used to calculated the averaged wavelet coefficient with the following formula [46]:

$$W[h] = \langle |W[h](a,b)| \rangle_b \tag{4}$$

The main point of this formula is to calculate the average wavelet at a given scale. Then average wavelet coefficient is plotted against scale a in a log-log plot. The slope of this line is $\frac{1}{2} + H$ and the spectral parameter is $\beta = 2H + 1$ [6, 27, 46].

2.3 Generation of $1/f^{\beta}$ fractal process

To begin the analysis of $1/f^{\beta}$ process, the first step is to generate a discrete $1/f^{\beta}$ fractal process as proposed by Papoulis [48] and improved by Hosking [49]. Generation of the random walk is proposed as the digital model [50]:

$$H_f(z) = \frac{1}{(1-z^{-1})^{\beta/2}} \tag{5}$$

The discrete $1/f^{\beta}$ fractal process is a pulse response function, and h_k associated with this model found by the transfer function [51]

$$H(z) = 1 - \frac{\beta}{2}z^{-1} - \frac{\beta/2(1-\beta/2)}{2!}z^{-2} + ... \tag{6}$$

The coefficients of the series of the discrete $1/f^{\beta}$ fractal process can be expressed with initial value $h_0 = 1$ and

$$h_k = \frac{(-\beta/2)_k}{k!} = \prod_{n=1}^{k} \frac{n-1-\beta/2}{n} \tag{7}$$

These values can be calculated by a recursive relation:

$$h_0 = 1 h_k = (k-1-\beta/2)\frac{h_{k-1}}{k} \tag{8}$$

The realization of x_n is the convolution operation between the pulse response values and Gaussian white noise [6].

2.4 Analysis description

Previous studies have shown that the mean stride intervals time series length in ten healthy control subjects is 3179 points for an hour of walking, considered to be a signal of sufficient length to calculate β, however, in a typical experiment, healthy subjects walk up to 15 minutes, which produce a time series about 600-900 time intervals. Data collected from unhealthy subjects such as those with pathological(ALS), Huntington's Disease(HD) and Parkinson's Disease(PD) are relatively shorter [6, 7]. An example of the total number and mean length of time series for each disease is listed in Table 1. It is clear that the patient population cannot provide a long stride interval time series.

2.4.1 Analysis of simulated intervals

In this part, we will generate $1/f^{\beta}$ processes and use AWC to estimate the value of β for different signal lengths. We considered $0 \leq \beta \leq 2$. The effect of non-zero mean does not need to be

considered [6], as AWC is sensitive to the choice of the mother wavelet and we will initiate our analysis with 16 commonly used mother wavelets. Next, the five most accurate mother wavelets will be chosen according to their global accuracy with different signal lengths, especially for short time series. The evaluation here examines the performance of these mother wavelets in the regime of the short time series ($N \leq 500$).

In the first step, $1/f^{\beta}$ signals are simulated for 100, 500, 1000, and 2000 points. At each signal length, $1/f^{\beta}$ signals with β fixed are repeated by 500 times. The interval of β used to generate the fractal process is [0,2] with an increment of 0.1. The mean square value (MSE) between the true β value and its estimated values is calculated.

Next, to mimic real physiological signals, $1/f^{\beta}$ signals are simulated for 100, 200, 300, 400, 500 and 600 points. We repeated the analysis as in the previous paragraph, but this time, we used $\beta \in [0, 2]$ with an increment of 0.01, and 1000 realizations for each β value. We compared the results previously obtained in [6] with the results obtained from the five mother wavelets.

2.4.2 Analysis of real stride interval data

Lastly, we reexamined the published data sets resulting from an investigation of gait dynamics in neurodegenerative diseases. The data for this examination consists of two parts, the first part was obtained by Haussdorf [3, 4, 7] in a study of stride interval correlations in both healthy people and in those with pathological diseases. These data include 13 ALS patients, 20 HD patients, 15 PD patients, and 16 healthy subjects. Only the right foot stride interval time series is considered for the calculation. The second part is from [52], which includes strides from 16 healthy patients. Figure 2 shows the sample of some stride interval data. The purpose of this evaluation is to examine the performance of different mother wavelets for the real short time series. Figure 2 shows stride interval samples from different types of subjects.

Table 1: Number of time Series and mean length, Study II. ALS = Amyotrophic Lateral Sclerosis, HD = Huntington's Disease, PD = Parkinson's Disease, CO = Control, CO2 = Second Control

	ALS	**HD**	**PD**	**CO**	**CO2**
Number of Series	13	20	15	16	16
Mean Length	196	242	184	255	842

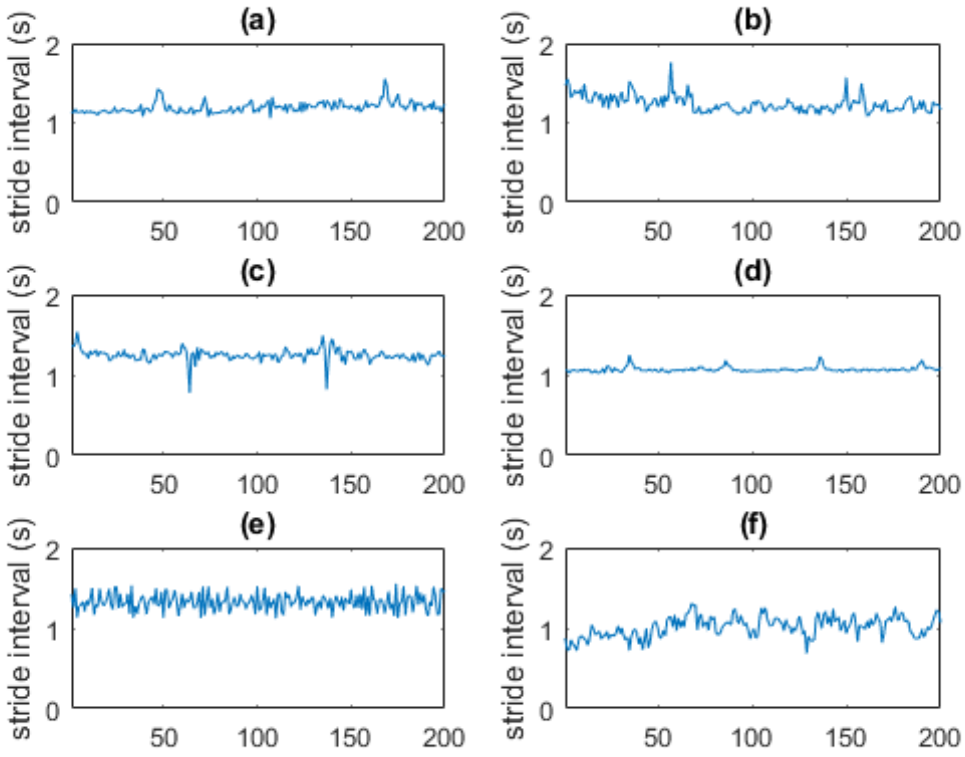

Figure 2: Samples of real data:(a) ALS (b) HD (c) PD (d) CO (e) CO2 (f) simulated signal

3 Results

The results of our numerical analysis are presented in this section. Firstly, the results from sixteen different mother functions are examined. Based on these results, five mother wavelet candidates were chosen for more detailed simulations. The goal of second part is to indicate which of the mother functions can most effectively evaluate the fractal nature of the time series for different signal lengths. Lastly, we compared the results of our five mother wavelet candidates with the results previously reported [6].

3.1 Overall performance of sixteen mother wavelets

The first part is the estimation accuracy of algorithm for $0 \leq \beta \leq 2$. Figure 3 shows the performance of sixteen mother wavelets, which calculate the mean-square-error of β of 500 random fractal signals with length varying from 100 to 2000 points.

The results indicate that the accuracies of the respective mother wavelets variy with different

Table 2: List of Acronyms

cgau	Complex Gaussian wavelet
sym	Symlets wavelet
db	Daubechies wavelet
bior	BiorSplines wavelet
mexh	Mexican hat wavelet
dmey	DMeyer wavelet
meyr	Meyer wavelet
morl	Morlet wavelet
rbio	Reverse bioorthogonal wavelet

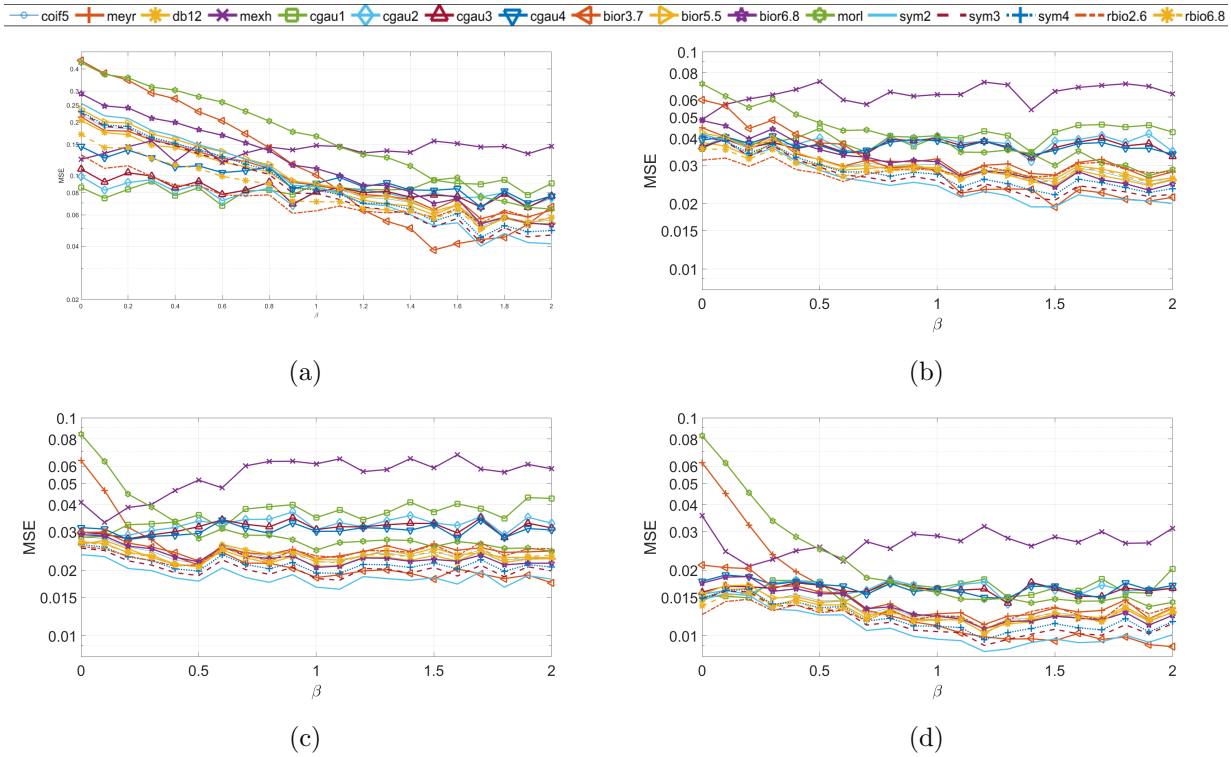

Figure 3: MSE of all mother wavelets (a) N=100; (b) N=500; (c) N=1000; and (d) N=2000.

β and signal length. For a short signal length, it is clear that cgau families provide more robust performance between $0 \leq \beta \leq 2$, while other mother wavelets display high mean squared errors (MSEs) for $\beta \leq 1$. Bior 3.7 shows very high MSE for the fGn class and very small MSE for the fBm class. Similar errors in the fGn class are found for the sym family and rbio family, and the

MSE decreases for $\beta > 1$. The morl and mexh mother wavelet give the relatively highest MSE for all cases. The other commonly used mother wavelets such as dmey, meyr, coif all yielded the relatively flat MSE across the range of β.

Considering the case of time series with a length of 500 points as given in Figure 3, it is clear that mexh mother function has significantly higher MSE for the entire range of β. In this case, cgau families still provide flat MSE across the range of β. Conversely, the results show that MSE is relatively high. Sym families provide better MSE compared to other mother wavelets, as MSE decreases as the signals type approaches to $\beta = 2$. Bior 3.7 mother wavelet gives a high MSE when β approaches to 0 and a small MSE when β approaches to 2.

In the case of time lengths of 1000 points and 2000 points, morl and meyr mother wavelets give very high MSE for fGn class. Mexth mother function demonstrates very high MSE for both the fGn class and fBm class. The rest of the mother wavelets shows similar results in which the MSE are relatively flat. Sym families demonstrate higher accuracy than any other mother functions.

3.2 Comparison of five mother wavelets

The analysis and comparison of the sixteen mother wavelets shows that the accuracy of those mother wavelets is not obvious. The selection of five mother wavelets is based on their performance for both long and short signals. For long signals, sym and bior shows better MSE results for both fBm and fGn class. For short signals, cgau1 and rbio2.6 show better accuracy than others for fGn class, sym and bior have good results for fBm class. As the real data is relatively short, we consider these five mother functions as our candidate functions.

MSE for the five mother wavelets As can be seen in Figure 4, sym2, sym3 and bior3.7 mother function demonstrate similar profiles as β increases. For these mother functions, higher MSE can be noted while β approaches 0, lower MSE is exhibited for the fBm class. In the case of 100 points and 200 points, cgau1 and rbio2.6 gives better MSE than others for analyzing the fractal signal with $\beta < 1$, however, they provide worse accuracy while signal length is over 200 points. Among all cases, rbio2.6 mother wavelets show better accracy for the fGn class, while better accuracy for fBm class is offered by sym2 mother function.

Mean Absolute Error (MAE) of the wavelets The results from five mother wavelets show that sym2 and db12 mother wavelets are the two best resolution in symlet and Daubechies wavelet famlies, and that cgau1 is the best resolution in cgau family when the time interval is short. rbio2.6 mother wavelet provides the most flat results in rbio family. Mean absolute error (MAE), bias,

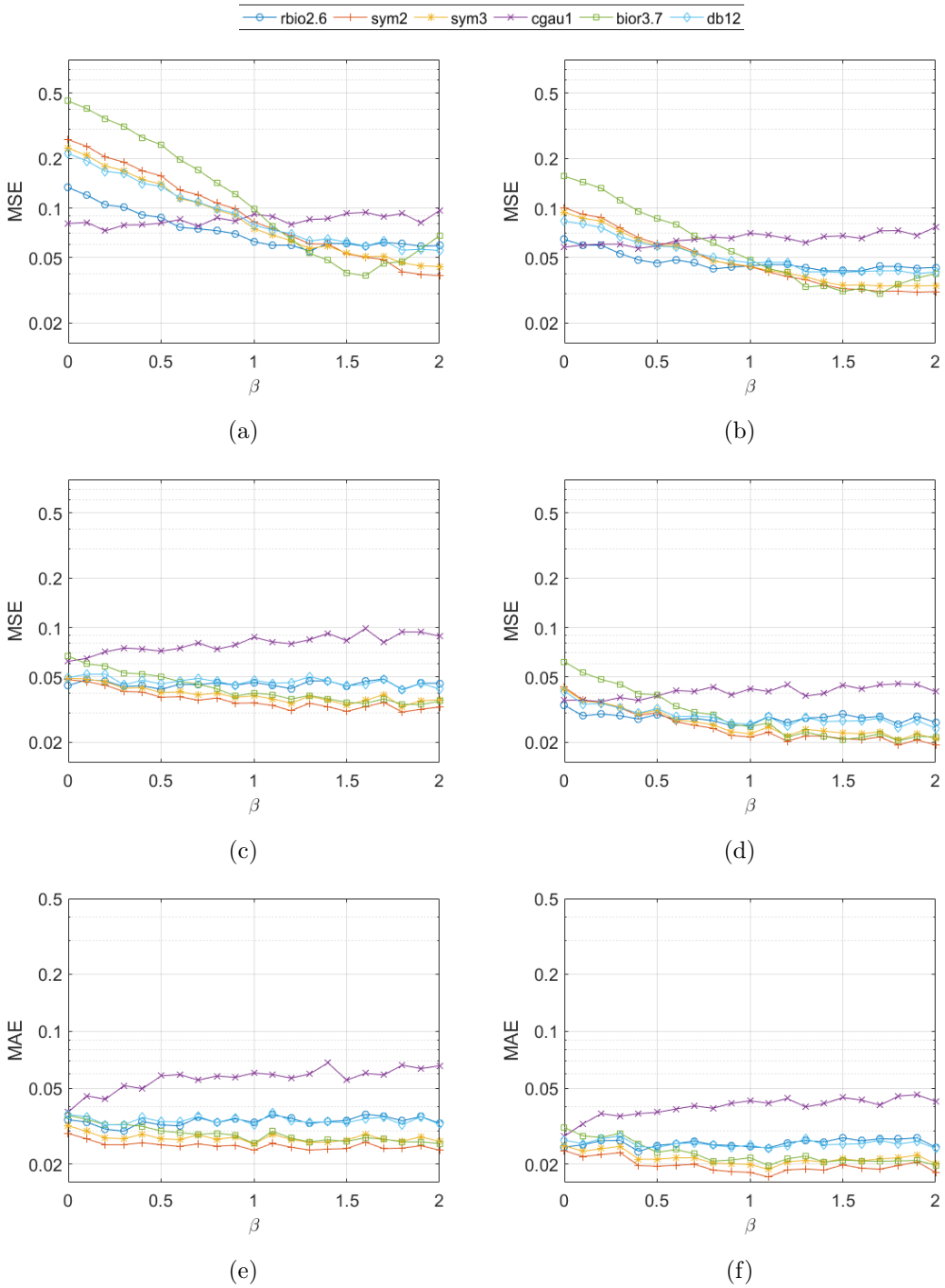

Figure 4: MSE of five mother wavelets and db12 mother wavelet (a) N=100; (b) N=200; (c) N=300; (d) N=500 ; (e) N=700 and (f) N=900

and variance will be examinaed using these five mother wavelet in the following figures. Figure 5 shows that the results of MAE from these five mother wavelets candidates are similar to their MSE results. The mean absolute error of cgau1 is flatter and lower than that of both sym2 and db12 for the fGn class when the time series are very short. When the time series increases, the MAE of sym2 and db12 tends to become smaller than that of cgau1. Sym2 mother wavelet always provides a lower mean absoulute error than do the db12 and rbio2.6 mother wavelets while $\beta > 1$ and the MAE decreases while β increases. bior 3.7 mother wavelet has the worst performance in the fGn class.

Bias and variance of the wavelets The MSE can be written as the sum of the squared bias and the variance [53]. The bias (mean error) and variance (standard deviation) will be examined separately in order to distinguish the different effects of three mother wavelets on bias and variance. Figure 6 indicates the bias of five mother wavelets on the range $0 \leq \beta \leq 2$ with signal lengths of 100 and 300. As can be seen in the figure, the mean error (bias) of cgau1 is lower than that of the other two mother wavelets at fGn regime when time series is around 100 points. db12 and rbio2.6 mother wavelets show a very low mean error when β is around 1 and the time series has 300 points. bior 3.7 provides the lowest mean error when β is around 1.6. The bias of sym2 decreases with the augmentation of the fractal exponent β. Figure 7 shows the variance of five mother wavelets. For all five mother wavelets, the variances remain relatively unchanged, which is the advantage of the AWC method [42]. Among all three mother wavelets, sym2 provides the lowest variance in the entire range of β, while cgau1 gives the highest variance. From these figures, we can find that compared to db12 and rbio2.6, sym2 gives a relatively high bias but low variance.

3.3 Stride interval analysis of numerical data

This section presents the results of the average wavelet coefficient methods applied to the measured gait stride interval time series. Due to the physical limitations of the patients in the considered

Table 3: Analysis of the algorithms for time series

	CO	**HUNT**	**PARK**	**ALS**	**CO2**
sym2	1.13±0.16	0.65±0.38	0.95±0.36	1.10±0.27	0.22±0.16
db12	1.04±0.19	0.55±0.41	0.88±0.40	1.03±0.27	0.18±0.19
cgau1	0.45±0.46	0.39±0.32	0.66±0.38	0.86±0.27	0.36±0.25
bior3.7	1.21±0.19	0.70±0.44	1.03±0.40	1.21±0.30	0.18± 0.18
rbio2.6	1.03±0.21	0.54±0.38	0.85±0.39	1.01±0.31	0.21±0.17

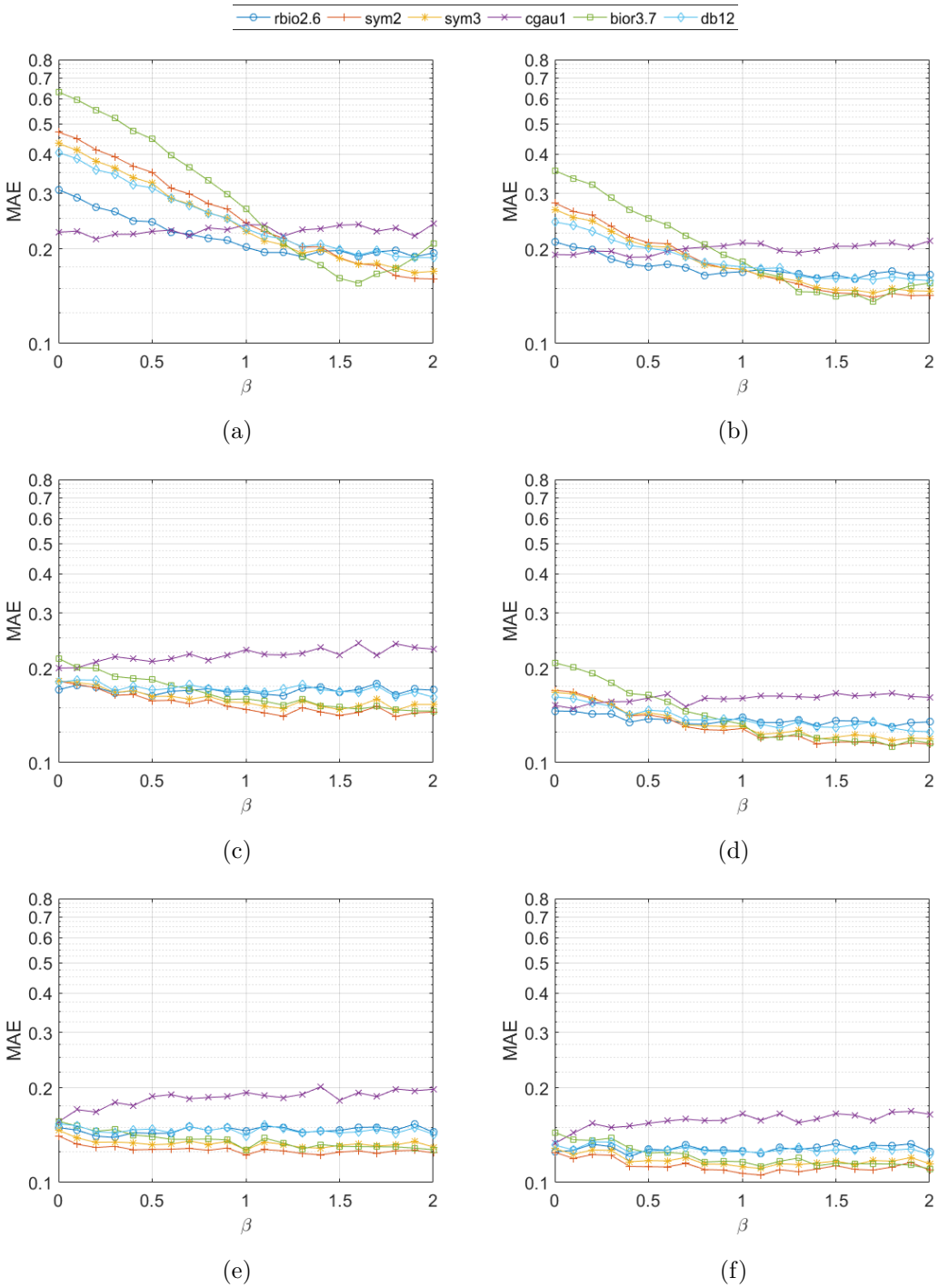

Figure 5: Mean absolute error vs β, (a) N=100; (b) N=200; (c) N=300; (d) N=500 ; (e) N=700 and (f) N=900

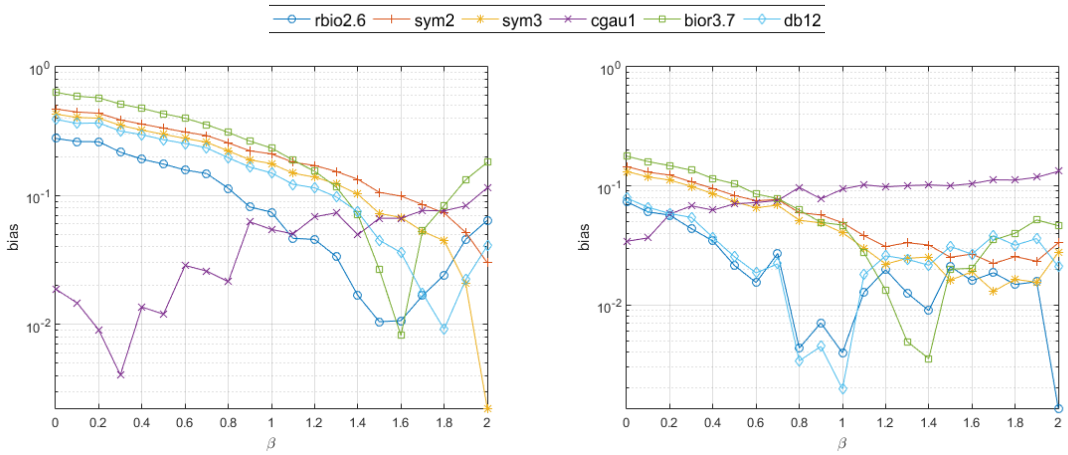

(a) (b)

Figure 6: Bias vs β, (a) n=100 (b) n=300

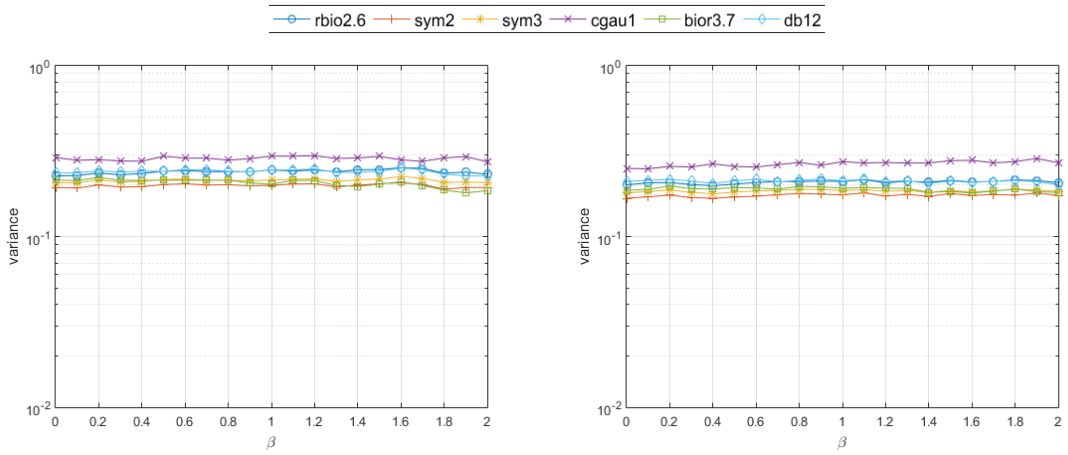

(a) (b)

Figure 7: Variance vs β, (a) n=100 (b) n=300

studies, the time series length is relatively short, as shown in Table 1. The spectral exponent β is calculated by AWC with cgau1, sym2, rbio2.6, bior3.7 and db12 mother wavelets. Table 3 shows the calculated β values (mean $\pm$ standard deviation) and Table 4 reveals p-values among different groups using the sym2 mother wavelet. As shown in Table 3, the standard deviation of all mother wavelets are very close which corresponds to the simulated results. Results show that mean results estimated by using cgau1 significantly differ from estimated values obtained by other mother wavelets. Most groups can be statistically differentiated (except CO/PD and CO/ALS) as shown in Table 4.

Table 4: P values among estimated β results from different groups using sym2 mother wavelet.

	CO2	PD	ALS	HUNT
CO	< 0.01	0.16	0.227	< 0.01
CO2		< 0.01	< 0.01	< 0.01
PD			0.043	0.045
ALS				0.01

4 Discussion

Based on the results of the numerical analysis of these different mother functions, it can be stated that each mother wavelet has distinct limitations and benefits. As the AWC method is not influenced by non-zero mean signals [6], it is critical to consider the time series length and the β value. The AWC method is a generally robust method, which has a more uniform performance for all ranges of β [6]. However, it is apparent that choosing a single suitable mother wavelet for all fractal nature process is quite untenable. It is obvious that the accuracy of the estimator increases with longer signal lengths. The $1/f^{\beta}$ power relationship can extend over decades of frequencies, while the data length strongly influences access to the spectral information at lower frequencies [33], and therefore seeking more data to analyze is the most efficient way to get more accurate results.

In reality, the data length is limited because of the difficulty of collection. For short time series, meyr, mexh, morl mother functions are clearly not suitable. The five best candidate functions were chosen to compare with the results from db12 as proposed by Simonson [46]. Cgau wavelet families show relatively flat MSE results for all cases that provide better accuracy for $\beta < 1$ within signal length of 200 points. The flat MSE results can also been seen in the rbio family for all signal lengths. Bior families and sym families illustrated in the change of β are similar. Bior wavelet families are biorthogonal wavelet parameterized by two numbers, and are therefore more computationally expensive [54]. The result given by db 12 mother wavelet performs inferiorly in comparison to sym2 for all β value and so does bior3.7 when $\beta > 1$.

The random fractal processes have the key property that they are invariant to temporal dilations and contractions of their processes and $1/f^{\beta}$ processes are statistically self-similar random processes that can be expanded in terms of orthonormal wavelets based on uncorrelated coefficients of the expansion. The orthonormal wavelet transform is a useful tool to analyze the $1/f^{\beta}$ process [33, 35,

55]. Generally, considering the real condition of physiological interest whose data length is between 200 to 400 points, sym2 is the most robust and suitable mother wavelet that provides the best accuracy.

The real data shows that results are largely affected by the time series length. In the simulation part, db12 has the lowest bias however sym2 mother wavelet gives a relatively lower variance (standard deviation) and a higher bias, which correspond to the results with real data. Compared with other mother wavelets cgau1 shows large differences in mean values and standard deviations. Results show great differences between CO and CO2 patients. The mean of CO subjects is around 1 for rbio2.6 and db12, and it is slightly higher than 1 for sym2 and bior3.7 mother wavelets. The mean of CO2 subjects is around 0.2 and the results are close to the results in the paper [52]. Both data sets are from healthy subjects, however, walks for subjects in the second data set were influenced by the equipment used in the study, which was main reason for lower β values.

Our results show that β values for ALS patients are around 1 which is close to the results yielded healthy control subjects [22]. The reason of this inference may be caused by the diversity of ALS patients. According to the Hausdorff paper, the group of ALS patients had a lot of variations in the major body region, and 4 patients exhibited the breathing problems [4]. The diversity of the disease status may influence these results.

5 Conclusion

We presented the use of the AWC based method for $1/f^{\beta}$ process analysis and proposed the most suitable mother wavelets for this purpose as applied to stride interval analysis in persons with neurological disorders. Often the gait data collected from patients is limited, therefore, the five candidate functions were applied to analyze the fractal process with short time series between 100 and 600 points. Primarily, the numerical analysis allowed us to preselect the five best mother wavelets from sixteen mother wavelets with different time series length. It was critical to choose a suitable mother wavelet with consistent accuracy and precision. From the simulated series, we conclude that the sym2 mother wavelet is numerically most suitable for analyzing physiological signals while considering the length of signals.

Acknowledgments

This work was supported in part by the Pittsburgh Claude D. Pepper Older Americans Independence Center (NIA P30 AG 024827).

References

[1] F. Steinicke and I. ebrary, *Human Walking in Virtual Environments: Perception, Technology, and Applications*, 1st ed. Springer, 2013.

[2] J. M. Hausdorff, C. K. Peng, Z. Ladin, J. Y. Wei, and A. L. Goldberger, "Is walking a random walk? Evidence for long-range correlations in stride interval of human gait," *Journal of Applied Physiology*, vol. 78, pp. 349–358, 1995.

[3] J. M. Hausdorff, L. Zemany, C. K. Peng, and A. L. Goldberger, "Maturation of gait dynamics: stride-to-stride variability and its temporal organization in children," *Journal of Applied Physiology*, vol. 86, pp. 1040–1047, 1999.

[4] J. M. Hausdorff, A. Lertratanakul, M. E. Cudkowicz, A. L. Peterson, D. Kaliton, and A. L. Goldberger, "Dynamic markers of altered gait rhythm in amyotrophic lateral sclerosis," *Journal of Applied Physiology*, vol. 88, no. 6, pp. 2045–2053, 2000.

[5] A. Arneodo, B. Audit, P. Kestener, and S. Roux, "Wavelet-based multifractal analysis," *Scholarpedia*, vol. 3, p. 4103, 2008.

[6] A. Schaefer, J. S. Brach, S. Perera, and E. Sejdić, "A comparative analysis of spectral exponent estimation techniques for $1/f^{\beta}$ processes with applications to the analysis of stride interval time series," *Journal of Neuroscience Methods*, vol. 222, pp. 118–130, January 2014.

[7] J. M. Hausdorff, S. L. Mitchell, R. Firtion, C. K. Peng, M. E. Cudkowicz, J. Y. Wei, and A. L. Goldberger, "Altered fractal dynamics of gait: reduced stride-interval correlations with aging and huntington's disease," *Journal of Applied Physiology*, vol. 82, p. 262, 1997.

[8] R. W. Glenny, H. T. Robertson, S. Yamashiro, and J. B. Bassingthwaighte, "Applications of fractal analysis to physiology," *Journal of Applied Physiology*, vol. 70, no. 6, pp. 2351–2367, 1991.

[9] J. B. Bassingthwaighte, L. S. Liebovitch, and B. J. West, *Fractal Physiology*. New York: Published for the American Physiological Society by Oxford University Press, 1994, vol. 2.

[10] A. Goldberger, "Non-linear dynamics for clinicians: chaos theory, fractals, and complexity at the bedside," *The Lancet*, vol. 347, no. 9011, pp. 1312–1314, 1996.

[11] J. M. Hausdorff, "Gait dynamics, fractals and falls: finding meaning in the stride-to-stride fluctuations of human walking," *Human Movement Science*, vol. 26, no. 4, pp. 555–589, 2007.

[12] ——, "Gait dynamics in Parkinson's disease: Common and distinct behavior among stride length, gait variability, and fractal-like scaling," *Chaos*, vol. 19, no. 2, 2009.

[13] A. Daffertshofer, "Persistent fluctuations in stride intervals under fractal auditory stimulation," *PloS one*, vol. 9, no. 3, p. e91949, 2014.

[14] J. B. Dingwell and J. P. Cusumano, "Re-interpreting detrended fluctuation analyses of stride-to-stride variability in human walking," *Gait and Posture*, vol. 32, no. 3, pp. 348–353, 2010.

[15] M. R. Daliri, "Chi-square distance kernel of the gaits for the diagnosis of Parkinson's disease," *Biomedical Signal Processing and Control*, vol. 8, no. 1, pp. 66–70, 2013.

[16] A. Vadnerkar, S. Figueiredo, N. E. Mayo, and R. E. Kearney, "Classification of gait quality for biofeedback to improve heel-to-toe gait," in *2014 36th Annual International Conference of the IEEE Engineering in Medicine and Biology Society*. IEEE, 2014, pp. 3626–3629.

[17] M. R. Daliri, "Automatic diagnosis of neuro-degenerative diseases using gait dynamics," *Measurement: Journal of the International Measurement Confederation*, vol. 45, no. 7, pp. 1729–1734, 2012.

[18] A. Khorasani, M. R. Daliri, and M. Pooyan, "Recognition of amyotrophic lateral sclerosis disease using factorial hidden Markov model," *Biomed Tech (Berl)*, vol. 61, no. 1, pp. 119–126, 2016.

[19] A. Khorasani and M. R. Daliri, "HMM for Classification of Parkinson's Disease Based on the Raw Gait Data," *Journal of Medical Systems*, vol. 38, no. 12, 2014.

[20] E. Baratin, L. Sugavaneswaran, K. Umapathy, C. Ioana, and S. Krishnan, "Wavelet-based characterization of gait signal for neurological abnormalities," *Gait and Posture*, vol. 41, no. 2, pp. 634–639, 2015.

[21] P. Ren, W. Zhao, Z. Zhao, M. L. Bringas-Vega, P. A. Valdes-Sosa, and K. M. Kendrick, "Analysis of gait rhythm fluctuations for neurodegenerative diseases by phase synchronization and conditional entropy," *IEEE Transactions on Neural Systems and Rehabilitation Engineering*, vol. 24, no. 2, pp. 291–299, 2016.

[22] E. Sejdić and L. A. Lipsitz, "Necessity of noise in physiology and medicine," *Computer Methods and Programs in Biomedicine*, vol. 111, pp. 459–470, 2013.

[23] J. B. Bassingthwaighte and R. P. Bever, "Fractal correlation in heterogeneous systems," *Physica D: Nonlinear Phenomena*, vol. 53, pp. 71–84, 1991.

[24] J. Bassingthwaighte, "Physiological heterogeneity: Fractals link determinism and randomness in structures and functions," *Physiology*, vol. 3, pp. 5–10, 1988.

[25] D. Delignieres, S. Ramdani, L. Lemoine, K. Torre, M. Fortes, and G. Ninot, "Fractal analyses for short time series: A re-assessment of classical methods," *Journal of Mathematical Psychology*, vol. 50, no. 6, pp. 525–544, 2006.

[26] S. G. Mallat, "A theory for multiresolution signal decomposition: the wavelet representation," *IEEE Transactions on Pattern Analysis and Machine Intelligence*, vol. 11, pp. 674–693, 1989.

[27] A. Eke, P. Herman, L. Kocsis, and L. R. Kozak, "Fractal characterization of complexity in temporal physiological signals," *Physiological Measurement*, vol. 23, no. 1, p. R1, 2002.

[28] D. Delignires and K. Torre, "Fractal dynamics of human gait: a reassessment of the 1996 data of hausdorff et al," *Journal of Applied Physiology*, vol. 106, no. 4, pp. 1272–1279, 2009.

[29] M. F. Schlesinger, "Fractal time and 1/f noise in complex systems," *Annals of the New York Academy of Sciences*, vol. 504, no. 1 Perspectives, pp. 214–228, 1987.

[30] N. J. Kasdin and N. J. Kasdin, "Discrete simulation of colored noise and stochastic processes and 1/f power law noise generation," *Proceedings of the IEEE*, vol. 83, no. 5, pp. 802–827, 1995.

[31] Y. Chen, M. Ding, and J. A. S. Kelso, "Long memory processes (1/f type) in human coordination," *Physical Review Letters*, vol. 79, no. 22, pp. 4501–4504, 1997.

[32] Y. Gao, M. J. Brennan, and P. F. Joseph, "A comparison of time delay estimators for the detection of leak noise signals in plastic water distribution pipes," *Journal of Sound and Vibration*, vol. 292, no. 3, pp. 552–570, 2006.

[33] G. Wornell, *Signal Processing with Fractals: A Wavelet-based Approach*, ser. Prentice Hall signal processing series. Prentice Hall PTR, 1996.

[34] B. B. Mandelbrot and J. W. Van Ness, "Fractional brownian motions, fractional noises and applications," *SIAM Review*, vol. 10, no. 4, pp. 422–437, 1968.

[35] G. W. Wornell, "Wavelet-based representations for the 1/f family of processes," *Proceedings of the IEEE*, vol. 81, no. 10, pp. 1428–1450, 1993.

[36] F. Crevecoeur, B. Bollens, C. Detrembleur, and T. M. Lejeune, "Towards a gold-standard approach to address the presence of long-range auto-correlation in physiological time series," *Journal of Neuroscience Methodsa*, vol. 192, pp. 163–172, 2010.

[37] M. Kale and F. B. Butar, "Fractal analysis of time series and distribution properties of hurst exponent," *Journal of Mathematical Sciences and Mathematics Education*, vol. 5, no. 1, pp. 8–19, 2011.

[38] M. J. Cannon, D. B. Percival, D. C. Caccia, G. M. Raymond, and J. B. Bassingthwaighte, "Evaluating scaled windowed variance methods for estimating the hurst coefficient of time series," *Physica A: Statistical Mechanics and its Applications*, vol. 241, pp. 606–626, 1997.

[39] B. J. West and A. L. Goldberger, "Fractals in physiology and medicine," *The Yale Journal of Biology and Medicine*, vol. 60, pp. 421–435, 1987.

[40] R. W. Glenny, H. T. Robertson, S. Yamashiro, and J. B. Bassingthwaighte, "Applications of fractal analysis to physiology," *Journal of Applied Physiology*, vol. 70, pp. 2351–2367, 1991.

[41] H. E. Stanley, A. L. Goldberger, Z. R. Struzik, P. C. Ivanov, L. A. N. Amaral, M. G. Rosenblum, and S. Havlin, "Multifractality in human heartbeat dynamics," *Nature*, vol. 399, pp. 461–465, 1999.

[42] M. Keshner, "1/f noise," *Proceedings of the IEEE*, vol. 70, pp. 212–218, March 1982.

[43] L. A. Lipsitz, "Dynamics of stability: the physiologic basis of functional health and frailty," *The Journals of Gerontology. Series A, Biological Sciences and Medical Sciences*, vol. 57, pp. B115–B125, 2002.

[44] J. M. Hausdorff, Y. Balash, and N. Giladi, "Time series analysis of leg movements during freezing of gait in parkinson's disease: akinesia, rhyme or reason?" *Physica A: Statistical Mechanics and its Applications*, vol. 321, pp. 565–570, 2003.

[45] W. G. Morsi and M. El-Hawary, "The most suitable mother wavelet for steady-state power system distorted waveforms," in *Electrical and Computer Engineering, 2008. CCECE 2008. Canadian Conference on.* IEEE, 2008, pp. 000 017–000 022.

[46] I. Simonsen, A. Hansen, and O. M. Nes, "Determination of the Hurst exponent by use of wavelet transforms." *Physical Review E*, vol. 58, pp. 2779–2787, 1998.

[47] R. Thakur, "Analysis of orthogonal and biorthogonal mother wavelet using gaussian noise for image denoising," *International Journal of Application or Innovation in Engineering and Management*, vol. 12, 2013.

[48] A. Papoulis, *Probability, Random Variables, and Stochastic Processes*, 3rd ed. New York: McGraw-Hill, 1991.

[49] J. R. M. Hosking, "Fractional differencing," *Biometrika*, vol. 68, pp. 165–176, 1981.

[50] N. Kasdin and T. Walter, "Discrete simulation of power law noise," *Frequency Control Symposium, 1992. 46th., Proceedings of the 1992 IEEE*, no. 27-29, pp. 274–283, May 1992.

[51] N. Kasdin, "Discrete simulation of colored noise and stochastic processes and $1/f^{\alpha}$ power law noise generation," *Proceedings of the IEEE*, vol. 83, pp. 802–827, May 1995.

[52] E. Sejdić, A. Millecamps, J. Teoli, M. Rothfuss, N. Franconi, S. Perera, A. Jones, J. Brach, and M. Mickle, "Assessing interactions among multiple physiological systems during walking outside a laboratory: An android based gait monitor," *Computer Methods and Programs in Biomedicine*, vol. 122, no. 3, pp. 450–461, 2015.

[53] A. S. Kapadia, W. Chan, and L. A. Moye, *Mathematical Statistics with Applications.* Boca Raton, FL: Taylor and Francis/CRC Press, 2005, vol. 179.

[54] S. Rout, "Orthogonal vs. biorthogonal wavelets for image compression," Ph.D. dissertation, Virginia Tech, 2003.

[55] G. W. Wornell and A. V. Oppenheim, "Estimation of fractal signals from noisy measurements using wavelets," *IEEE Transactions on Signal Processing*, vol. 40, no. 3, pp. 611–623, 1992.

6 Appendix

Table 5 and Table 6 show mean and standard deviations of β values calculated from simulated signals.

Table 5: Mean and Standard deviation of estimated beta values with signal length n = 100

β	**rbio2.6**	**sym2**	**sym3**	**cgau1**	**bior3.7**	**db12**
0.1	0.36±0.22	0.55±0.19	0.51±0.21	0.12±0.28	0.7±0.21	0.47±0.23
0.2	0.44±0.23	0.62±0.2	0.58±0.21	0.23±0.29	0.75±0.21	0.54±0.24
0.3	0.52±0.24	0.69±0.21	0.65±0.22	0.29±0.28	0.81±0.23	0.62±0.25
0.4	0.58±0.24	0.75±0.2	0.72±0.21	0.4±0.29	0.87±0.22	0.68±0.25
0.5	0.68±0.23	0.84±0.2	0.8±0.21	0.5±0.29	0.94±0.21	0.77±0.24
0.6	0.75±0.23	0.91±0.2	0.87±0.21	0.58±0.29	0.99±0.22	0.84±0.24
0.7	0.84±0.24	0.99±0.2	0.96±0.21	0.67±0.29	1.06±0.21	0.93±0.24
0.8	0.9±0.24	1.05±0.2	1.02±0.22	0.75±0.28	1.11±0.22	0.99±0.25
0.9	0.99±0.24	1.13±0.2	1.1±0.21	0.85±0.29	1.16±0.22	1.07±0.25
1	1.09±0.24	1.22±0.2	1.19±0.21	0.96±0.28	1.24±0.2	1.17±0.24
1.1	1.16±0.24	1.3±0.2	1.26±0.21	1.06±0.3	1.3±0.21	1.24±0.25
1.2	1.25±0.24	1.37±0.2	1.34±0.21	1.15±0.29	1.34±0.21	1.31±0.24
1.3	1.33±0.23	1.45±0.19	1.42±0.2	1.22±0.29	1.41±0.2	1.39±0.23
1.4	1.41±0.24	1.53±0.2	1.5±0.21	1.32±0.28	1.47±0.21	1.47±0.25
1.5	1.51±0.24	1.62±0.2	1.59±0.21	1.44±0.28	1.54±0.19	1.57±0.24
1.6	1.58±0.26	1.69±0.21	1.66±0.23	1.53±0.29	1.59±0.21	1.63±0.25
1.7	1.67±0.24	1.77±0.2	1.74±0.22	1.61±0.29	1.65±0.19	1.71±0.24
1.8	1.77±0.23	1.87±0.19	1.84±0.2	1.72±0.29	1.71±0.19	1.8±0.23
1.9	1.85±0.24	1.95±0.19	1.92±0.21	1.82±0.27	1.76±0.19	1.88±0.23
2	1.95±0.23	2.04±0.19	2.01±0.2	1.92±0.29	1.83±0.18	1.97±0.22

Table 6: Mean and Standard deviation of estimated beta values with signal length n = 500

β	**rbio2.6**	**sym2**	**sym3**	**cgau1**	**bior3.7**	**db12**
0.1	0.18±0.16	0.24±0.13	0.23±0.14	0.1±0.19	0.28±0.15	0.2±0.16
0.2	0.28±0.16	0.34±0.13	0.33±0.14	0.19±0.19	0.37±0.14	0.3±0.16
0.3	0.37±0.16	0.43±0.13	0.42±0.14	0.27±0.21	0.46±0.15	0.39±0.16
0.4	0.46±0.16	0.51±0.13	0.5±0.14	0.38±0.2	0.54±0.15	0.48±0.16
0.5	0.54±0.16	0.6±0.13	0.59±0.14	0.47±0.2	0.62±0.15	0.56±0.16
0.6	0.64±0.17	0.69±0.14	0.68±0.15	0.57±0.2	0.71±0.15	0.66±0.17
0.7	0.74±0.17	0.79±0.14	0.78±0.15	0.67±0.21	0.79±0.15	0.75±0.17
0.8	0.83±0.17	0.88±0.14	0.88±0.15	0.76±0.2	0.89±0.15	0.85±0.17
0.9	0.93±0.16	0.97±0.14	0.97±0.15	0.86±0.19	0.98±0.15	0.94±0.16
1	1.02±0.16	1.06±0.14	1.06±0.14	0.97±0.2	1.06±0.15	1.03±0.16
1.1	1.11±0.17	1.16±0.14	1.15±0.15	1.06±0.19	1.15±0.15	1.12±0.17
1.2	1.22±0.17	1.26±0.14	1.25±0.15	1.17±0.21	1.25±0.15	1.23±0.16
1.3	1.3±0.17	1.35±0.14	1.34±0.15	1.26±0.2	1.33±0.15	1.31±0.17
1.4	1.41±0.16	1.45±0.13	1.44±0.14	1.36±0.2	1.41±0.14	1.41±0.16
1.5	1.51±0.17	1.54±0.14	1.54±0.15	1.45±0.2	1.51±0.14	1.51±0.16
1.6	1.6±0.17	1.64±0.14	1.63±0.15	1.56±0.19	1.59±0.15	1.6±0.16
1.7	1.71±0.16	1.74±0.13	1.73±0.14	1.65±0.2	1.69±0.14	1.71±0.16
1.8	1.79±0.17	1.83±0.14	1.82±0.15	1.77±0.2	1.78±0.15	1.8±0.16
1.9	1.91±0.17	1.94±0.14	1.93±0.14	1.86±0.2	1.87±0.14	1.9±0.16
2	2±0.17	2.03±0.14	2.02±0.14	1.96±0.21	1.96±0.14	2±0.16